Work Function on Dye-Adsorbed TiO2 Surfaces Measured by Using a Kelvin Probe Force Microscope

ARTICLE *in* THE JOURNAL OF PHYSICAL CHEMISTRY C · APRIL 2008

Impact Factor: 4.77 · DOI: 10.1021/jp077065+

5 AUTHORS, INCLUDING:

Naoki Koide
Sharp Corporation
53 PUBLICATIONS **3,303** CITATIONS
SEE PROFILE

Hiroshi Onishi
Kobe University
184 PUBLICATIONS **5,116** CITATIONS
SEE PROFILE

Work Function on Dye-Adsorbed TiO_2 Surfaces Measured by Using a Kelvin Probe Force Microscope

Masatoshi Ikeda,[†] Naoki Koide,[‡] Liyuan Han,[‡] Akira Sasahara,*[,†,§] and Hiroshi Onishi[†]

Department of Chemistry, Faculty of Science, Kobe University, Nada-ku, Kobe 657-8501, Japan, Sharp Corporation, Hajikami, Katsuragi, Nara 639-2198, Japan, and Japan Science and Technology Agency, Kawaguchi, Saitama 332-0012, Japan

Received: September 3, 2007; In Final Form: January 17, 2008

Work function measurements were conducted on Ru(4,4′-dicarboxy-2,2′-bipyridine)$_2$(NCS)$_2$ (N3 dye)-adsorbed titanium dioxide (TiO_2) surfaces by using a Kelvin probe force microscope. A rutile TiO_2(110)-(1 × 1) surface covered by a pivalate anion monolayer was immersed in acetonitrile containing N3 dye. In topographic images, the N3 molecules which replaced the pivalate anions were observed as bright particles embedded in the pivalate monolayer. Work function maps obtained in the dark showed that work function on the N3 molecules was larger by 0.07 eV than that on the surrounding pivalate monolayer. When measured under visible light irradiation, the work function on 44% of the N3 molecules reduced by 0.14 eV. We assume that the adsorbed molecules provide electric dipole moments to perturb the work function. The reduced work function indicates that the dipole moment directed from the surface to the vacuum is enhanced by the irradiation. Electron injection from N3 molecules to the surface is proposed to originate the photoinduced dipole moment.

1. Introduction

Solar cells employing a dye-sensitized semiconductor as the electrode provide a promising substitute for existing silicon-based cells due to low production costs and potentially high solar-to-electric energy conversion efficiency.[1,2] Electrons photoexcited in dye molecules are transferred to an external circuit through a semiconducting film. To date, over 11% energy conversion efficiency has been attained,[3] but further improvements are required for public use.

Electron transport at the dye−semiconductor interface is a key step in the energy conversion process.[4,5] The electron passes through overlapping molecular orbitals of the dye and semiconductor surface. Electron transport should therefore be sensitive to the structure of the dye. The surface density of states of the semiconductor is also sensitive to local structures including step, vacancies, and so forth. Electron transport efficiency is thus controlled by how and where the dye is adsorbed over the surface. However, there has been no way to know the electron transport properties of individual dyes. We recently proposed the application of scanning probe microscopy in characterizing individual adsorbed dyes and succeeded in topographic imaging of retinoate[6] and N3[7] on titanium dioxide (TiO_2).

In this study, work function imaging is achieved with a molecular resolution on dye-adsorbed TiO_2 surfaces in an attempt to monitor the light-induced electron transport. A photoinduced reduction of work function is observed on some dyes and related to the electron injection, by assuming the local work function affected by the electric dipole moment.

* To whom correspondence should be addressed. E-mail: sasahara@jaist.ac.jp. Present address: School of Materials Science, Japan Advanced Institute of Science and Technology, 1-1 Asahidai, Nomi, Ishikawa 923-1292, Japan.

[†] Kobe University.

[‡] Sharp Corporation.

[§] Japan Science and Technology Agency.

2. Kelvin Probe Force Microscope

Work function measurements were carried out by using a Kelvin probe force microscope (KPFM).[8,9] The KPFM is an extension of the noncontact atomic force microscope (NC-AFM),[10] and it provides a potential map of a solid surface simultaneously with its topography. The lateral resolution of the potential map reaches atomistic scales.[11−17] The NC-AFM is a scanning probe microscope which employs a weak attractive force to regulate the tip−sample distance. A cantilever with a tip at the free end is oscillated at its resonant frequency, and the force acting on the tip is detected as a shift of the resonant frequency (Δf). In the KPFM measurement, the contact potential difference (CPD) between the tip and surface is determined by measuring the electrostatic force F_{el}. The F_{el} acting on the tip is given by the following equation.

$$F_{el} = -\frac{1}{2}\frac{\partial C}{\partial z}\left(\frac{\Delta\Phi}{e}\right)^2 \quad (1)$$

where e, C, and $\Delta\Phi$ are the electron charge, the capacitance between the tip and surface, and the work function difference of the tip and surface, respectively. When a modulated bias voltage $V_{DC} + V_{AC}\sin(\omega t)$ is applied between the tip and surface, F_{el} is given by

$$\begin{aligned} F_{el} &= -\frac{1}{2}\frac{\partial C}{\partial z}\left\{\frac{\Delta\Phi}{e} - (V_{DC} + V_{AC}\sin(\omega t))\right\}^2 \\ &= -\frac{1}{2}\frac{\partial C}{\partial z}\left\{\left(\frac{\Delta\Phi}{e} - V_{DC}\right)^2 + 2\left(\frac{\Delta\Phi}{e} - V_{DC}\right)V_{AC}\sin(\omega t) + \frac{{V_{AC}}^2}{2}(1 - \cos(2\omega t))\right\} \end{aligned} \quad (2)$$

The local CPD is determined to be eV_{DC}, when the amplitude of F_{el} modulation with frequency ω is minimized. Here, we

10.1021/jp077065+ CCC: $40.75
Published on Web 04/08/2008

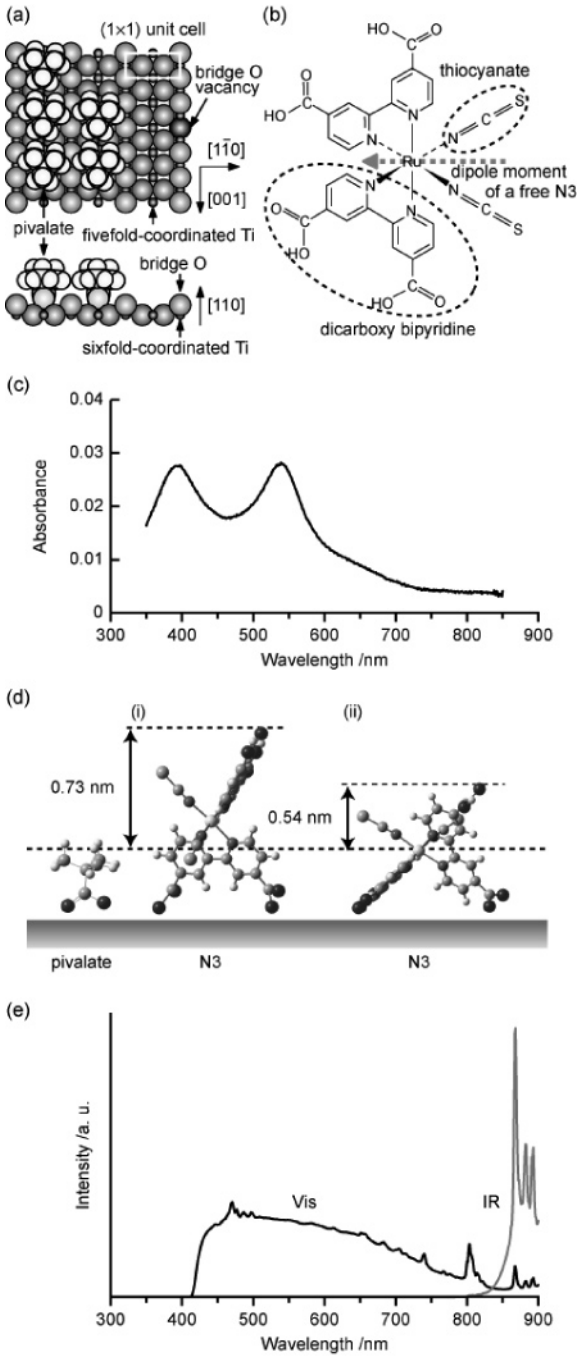

Figure 1. Models of (a) TiO_2(110)-(1 × 1) surface and (b) N3 molecule. The left side of the TiO_2 surface is covered by pivalate anions. (c) Absorption spectrum of our 0.02 mM acetonitrile solution of N3 dye. The optical path length was 1 mm. (d) Possible configurations of the pivalate and N3 adsorbed on a TiO_2(110)-(1 × 1) surface. Hydrogen atoms of the anchored carboxyl groups are removed, and the twist of the OCO planes relative to the pyridine ring planes is not included. (e) Spectra of incident visible light (black line) and infrared light (gray line).

use the local work function to show the direction of the potential shift unequivocally.

3. Model Electrodes

A rutile TiO_2(110) surface used as a substrate is depicted in Figure 1a.[18] The non-reconstructed (1 × 1) phase prepared in a vacuum consists of atomically flat terraces separated by steps with a height of 0.32 nm. On the terraces, fivefold-coordinated Ti atom rows and bridge O atom rows are extended to the [001] direction. The (1 × 1) surface is covered by a monolayer of pivalate ($(CH_3)_3CCOO^-$) anions for protection against the contaminants during the dye adsorption process. The pivalate anion, formed by dissociative adsorption of a pivalic acid ($(CH_3)_3CCOOH$), is anchored to two fivefold-coordinated Ti atoms in a bridge form with the OCO plane perpendicular to the surface.[19] The accompanying H atom is adsorbed on the bridge O atom. At the saturation coverage, the pivalate anions are densely packed with a (2 × 1) periodicity and form a stable monolayer exposing chemically inert alkyl groups at the topmost surface.

The dye examined is Ru(4,4′-dicarboxy-2,2′-bipyridine)$_2$-$(NCS)_2$, which is one of the most efficient sensitizer dyes reported to date[1] and is commonly called N3. As shown in Figure 1b, two bipyridine ligands and two thiocyanate ligands are coordinated to the ruthenium center with C_2 symmetry around the bisection of the ∠NRuN angle formed by the N atoms of the thiocyanate groups. The carboxyl groups (COOH) of the bipyridine ligands are used as anchors to the TiO_2 surfaces.[20,21] The ultraviolet−visible (UV−vis) light absorption spectrum of N3 in acetonitrile is presented in Figure 1c. The absorption band of N3 reaches 750 nm.

When the pivalate-covered surface is immersed in an acetonitrile solution of N3, N3 molecules replace the pivalate anions preadsorbed on the TiO_2(110) surface. The illustration in Figure 1d shows two possible configurations of the adsorbed N3 molecules that we proposed on the basis of the coordination of the carboxyl groups to the Ti sites of the (1 × 1) surface.[7] In the illustration, the distance between the O atoms of the anchored carboxyl group and the fivefold-coordinated Ti atoms is assumed to be 0.20 nm for N3 following a quantum mechanical calculation study of bi-isonicotinic acid.[22] The O−Ti distance of the pivalate is 0.21 nm following an X-ray photoelectron diffraction study of the formate ($HCOO^-$) anion.[23]

4. Experimental Procedures

An ultrahigh vacuum microscope (JSPM4500A, JEOL) equipped with a KPFM driver (TM-26030, JEOL), an ion sputtering gun (EX03, Thermo), and low-energy electron diffraction optics (BDL600, OCI) was used. The base pressure of the microscope chamber was 2×10^{-8} Pa.

A TiO_2(110) wafer (7 × 1 × 0.3 mm^3, Shinko-sha) was cleaned by cycles of Ar^+ sputtering and vacuum annealing at 1100 K. The temperature monitored by an optical pyrometer was overestimated because the temperature of the Si heater was observed through the transparent TiO_2 wafer. The obtained (1 × 1) surface was exposed to 900 L (1 L = 1×10^{-6} Torr s) of pivalic acid vapor at room temperature. The pivalic acid was purified by a freeze−pump−thaw cycle beforehand and was introduced into the vacuum chamber through a leak valve. The pivalate-covered TiO_2 wafer was removed from the vacuum chamber and immersed in acetonitrile containing N3. The immersed wafer was rinsed with pure acetonitrile and reintroduced into the microscope chamber.

Scanning tunneling microscope (STM), NC-AFM, and KPFM measurements were separately performed at room temperature by using n-type Si cantilevers (NSC35, MikroMasch) as probes. The experimentally determined resonant frequency of the cantilevers was about 300 kHz, and the nominal spring constant and phosphorus dopant concentration were 14 N/m and 10^{17} cm^{-3}, respectively. The tip was occasionally cleaned by Ar^+ sputtering. The STM images were acquired in the constant-current mode with positive sample bias voltages. Simple NC-AFM topography was acquired with the constant frequency-

shift mode. The sample bias voltage (V_s) was optimized to provide high-contrast topography with a minimum frequency shift. In KPFM operation, the frequency and peak-to-peak amplitude of the modulation bias voltage were 2 kHz and 2 V, respectively. Physically protruded places are presented as bright in the topography, and places with large work function are presented as bright in the work function map. The images were captured with a resolution of 512 × 512 pixels and presented as raw images.

A 300 W Xe arc lamp (CX-04E, Eagle Engineering) was used as a light source. A sharp cut filter (L-42, HOYA) and heat absorption filter (HA-50, HOYA) were inserted for visible light irradiation. An infrared transmitting filter (IR-85, HOYA) was used for infrared light irradiation. The incident light spectrum was estimated from the emission spectrum of the Xe arc lamp in the specification sheet and experimentally determined transmissivity of the filters as shown in Figure 1e. The filtered light was introduced to the sample surface with an incident angle of 45° through a quartz viewport. The visible light intensity at the sample surface was estimated to be 1.5 mW cm^{-2}.

5. Results and Discussion

5.1. STM and NC-AFM Imaging of the Surfaces. Isolated and aggregated N3 molecules should provide different properties. To identify which molecule is isolated or aggregated, the N3-adsorbed TiO_2 surfaces were carefully examined by using the STM and NC-AFM. Figure 2a is an STM image of the TiO_2 surface exposed to pivalic acid gas. The spots arranged in a (2 × 1) periodicity are pivalate anions. The pivalate monolayer provides a periodic topography as the cross section A in Figure 2d shows. Two terraces are separated by a step with a height of 0.32 nm, which is similar to the single step height of the uncovered surface. The bright particle indicated by the arrowhead is the TiO_x species formed during the surface preparation. The number density of the TiO_x species was less than 0.01 nm^{-2}.

By immersing in a 0.02 mM N3 solution for 2 min, bright particles appeared with a number density of 0.07 nm^{-2} as shown in Figure 2b. The particles increased in number with the immersion time and were therefore assigned to the N3 molecules which replaced the pivalates. The particles with a minimum diameter of 2.0 nm were assigned to isolated N3 molecules. The cross section B in Figure 2d passes through the center of an isolated N3 molecule. Particles of larger lateral size are aggregated N3 molecules, though individual N3 molecules are not resolved. The fraction of isolated N3 molecules was 0.32 relative to all the particles.

The heights of 148 isolated N3 molecules ranged from 0.25 to 1.10 nm relative to the pivalate monolayer as shown in Figure 2e. The height distribution was wider than that obtained in our previous study,[7] which is presumably due to tips of different sharpness. The average height of the isolated N3 molecules was 0.57 nm and was interpreted on the two adsorption configurations (i) and (ii). The spatial distribution of the lowest unoccupied molecular orbital (LUMO) of the N3 molecule[24] was considered there. The height of the aggregates was distributed from 0.25 to 1.10 nm and was 0.63 nm on average.

In Figure 2, image c shows an NC-AFM image of the surface of image b. N3 molecules were observed as particles with a number density of 0.05 nm^{-2}, and the isolated N3 molecules were identified as the particles with a minimum diameter of 3.0 nm. The number ratio of the isolated N3 molecules to all the particles was 0.35, being comparable to the fraction observed

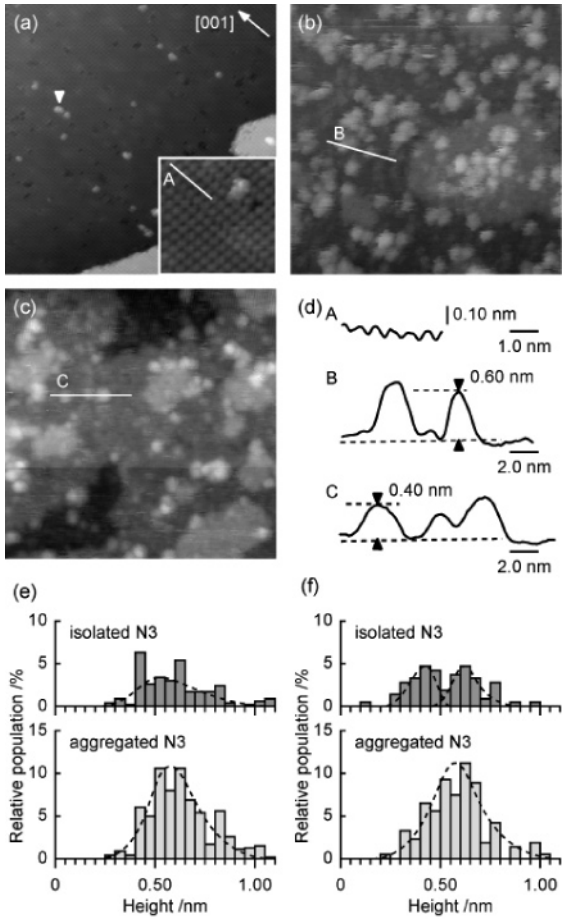

Figure 2. STM images of a pivalate-covered TiO_2(110) surface (a) before and (b) after immersion in 0.02 mM N3/acetonitrile solution for 2 min (50 × 50 nm^2). A narrow-scan image (7.5 × 7.5 nm^2) is inset in (a). Sample bias voltage $V_s = +1.0$ V; tunneling current $I_t =$ 1.0 nA. (c) NC-AFM image of the pivalate-covered TiO_2 surface immersed in 0.02 mM N3/acetonitrile solution for 2 min (50 × 50 nm^2). Frequency shift $\Delta f = -107$ Hz, $V_s = 0$ V, and peak-to-peak amplitude of the cantilever oscillation (A_{p-p}) = 6.0 nm. (d) Cross sections determined along the lines in the images. (e) Height of the particles relative to the pivalate monolayer in STM images. (f) Height of the particles relative to the pivalate monolayer in NC-AFM images. Dashed lines help guide the eye.

in the STM images. The height distribution of 75 isolated N3 molecules presents two peaks at 0.40 and 0.60 nm, as shown in Figure 2f. The number ratio of the small and large particles was approximately 1. The height of the N3 aggregates ranged from 0.20 to 1.05 nm and had an average of 0.58 nm.

The two species found in the isolated N3 molecules may reflect different adsorption configurations. However, it is currently difficult to estimate the conformation on the basis of the constant frequency-shift topography. The tip−molecule force detected by the microscope is the mixture of van der Waals forces,[25] electrostatic forces due to the dipole moment in the molecule,[26] and chemical forces, if any.

5.2. KPFM Measurements in the Dark. Figure 3a and b shows the topography and work function map of the N3-adsorbed TiO_2 surface observed in the dark. Cross sections obtained along the lines in the images are presented in Figure 3c. In the topography, N3 molecules were observed as bright particles with a number density of 0.04 nm^{-2}. The particles with a minimum diameter of 2.0 nm are assigned to isolated N3 molecules, and the number ratio of the isolated to the whole particles was 0.23. The number density and fraction of the

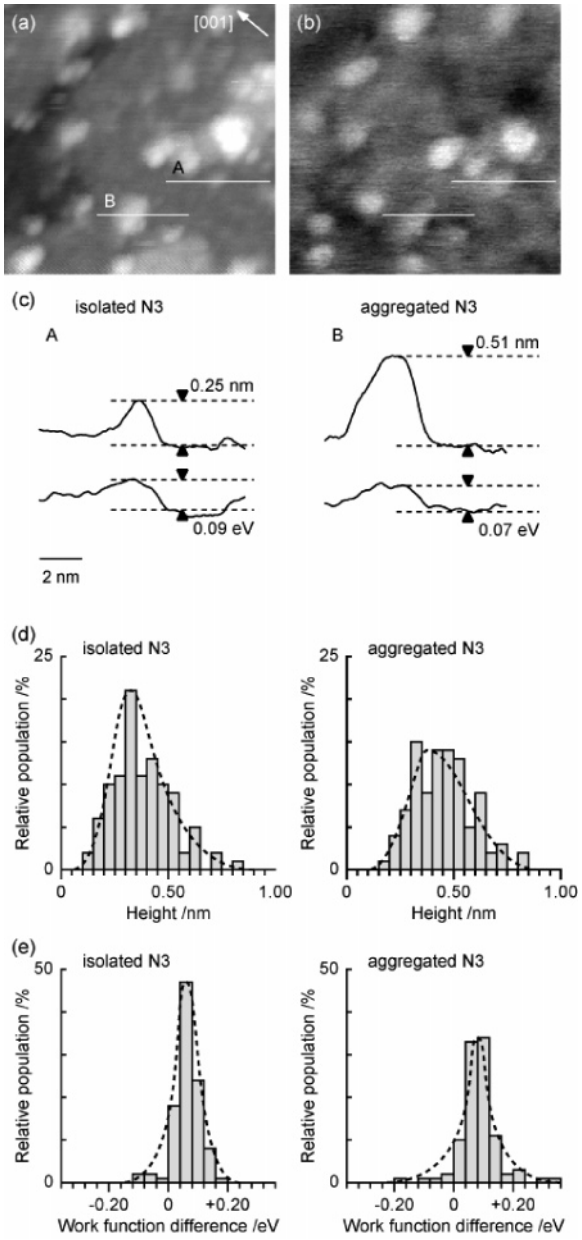

Figure 3. (a) Topography and (b) work function maps of the N3-adsorbed TiO_2 surface obtained in the dark (30×30 nm^2). $\Delta f = -70$ Hz, and $A_{p-p} = 6.2$ nm, $v_s = 3.3$ ms/pixel. (c) Cross sections determined along the lines in the images. (d) Heights of the single N3 molecules and the N3 aggregates relative to the pivalate monolayer in the topography. (e) Work function shift on the N3 molecules. Dashed lines help guide the eye.

isolated particles are similar to those determined from the STM and NC-AFM images.

The height distribution of 131 isolated N3 molecules ranged from 0.1 to 0.8 nm as shown in Figure 3d. The wide distribution of the isolated N3 molecules may reflect the difference in the adsorption configuration. The topographic height of the isolated and also aggregated N3 molecules was reduced compared with those obtained in the NC-AFM images (Figure 2). The tip approached closer to the N3 molecules because the long-range electrostatic interaction was minimized in the KPFM imaging.

In the work function map, the adsorbed N3 molecules are presented as bright particles, where the local work function is larger than that on the pivalate monolayer. The distribution of the local work function shift is presented in Figure 3e. The work function shift of the isolated N3 molecules is distributed from +0.2 to 0.0 eV with an averaged shift of +0.07 eV. The work function shift of the aggregated N3 molecules is still positive and more widely distributed than that of the isolated molecules. The widely distributed work function of the aggregated N3 molecules is because of possible heterogeneity of N3 molecules in the aggregates. The observed work function shifts were well over experimental uncertainty.

The pivalate anion on the TiO_2(110) surface provides a dipole moment perpendicular to the surface directed from the surface to the vacuum. The work function of the surface reduces by 0.8 eV as a result of the pivalate adsorption.[27] The strength of the dipole moment is estimated to be 0.8 debye per pivalate, by assuming that the monolayer of a number density of 2.6×10^{14} pivalate cm^{-2} provides a parallel plate condenser. The estimated strength is comparable to that of the formate anion adsorbed on this TiO_2 surface (0.9 debye).[28] Hence, the dipole moment of the adsorbed pivalate and formate is attributed to the COO^- group bound to the TiO_2 surface, a common structure of the two adsorbates.

The dipole moment of the free N3 molecule calculated by the density functional theory method is 10.9 debyes and is directed from the NCS ligands to the bipyridine ligands along the C_2 axis,[24] as illustrated in Figure 1b. When the dipole moment of the free N3 molecule is simply put on the surface in configurations (i) and (ii), the surface normal component of the moment is directed from the vacuum to the surface. The magnitude of the normal component is estimated to be 6 and 5 debyes.

The larger work function on the N3 molecules seems to be explained by the directions of the dipole moments originated from the pivalate and the N3 molecules. However, the observed work function increment by 0.07 eV means that the N3 molecule decreases the work function by 0.73 eV despite the assumption that the surface normal component of the dipole moment originated from the N3 molecule was directed to the surface. The experimental and theoretical accounts contradict here. To explain the work function increase on the N3 molecule, structural distortion of the N3 molecule by the adsorption has to be taken into account. The structure optimization in a density functional theory calculation predicted a significant distortion of the N3 molecule and relaxation of the TiO_2 surface atoms.[29]

5.3. KPFM Measurements under Visible Light Irradiation. The topography and the work function map of the N3-adsorbed surface obtained under visible light are presented in Figure 4a and b. The cross sections obtained along the lines in the images are shown in Figure 4c. In the topography, isolated N3 molecules with a minimum lateral size of 2.0 nm and aggregates of larger sizes were identified. The number density of the isolated and aggregated N3 molecules was 0.05 nm^{-2}, and the number ratio of the isolated molecules was 0.29. The number density and the number ratio were comparable to those observed in the dark. This does not suggest desorption or degradation of N3 by light irradiation. The height distribution of 120 isolated N3 molecules ranged from 0.1 to 0.8 nm and showed two distinct peaks at 0.3 and 0.4 nm. The peak at 0.3 nm was present in the dark, whereas the peak at 0.4 nm appeared by irradiation. The newly appeared peak suggests a structural change of the N3 molecules by light irradiation. The N3 aggregates exhibited a distribution between 0.1 and 0.8 nm with a concentration at 0.4 nm, being similar to that observed in the dark.

Obvious shifts by irradiation were found in the local work function. Some N3 molecules are displayed as depressions in the work function map shown in Figure 4b; that is, the work

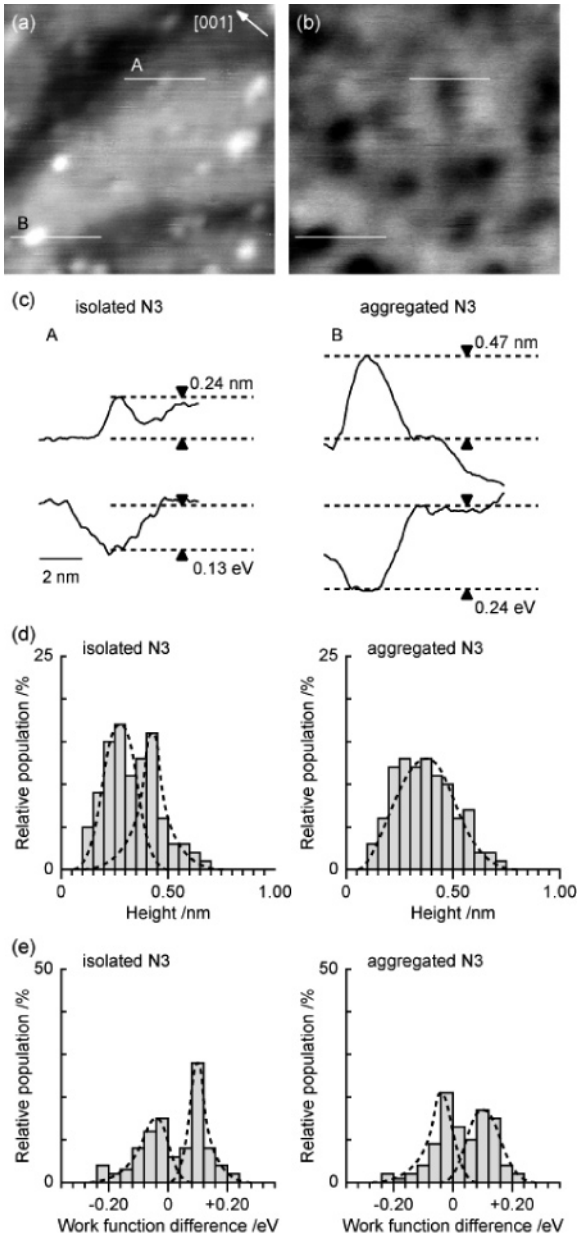

Figure 4. (a) Topography and (b) work function maps of the N3-adsorbed TiO_2 surface obtained under visible light of 1.5 mW cm^{-2} intensity (30 × 30 nm^2). $\Delta f = -70$ Hz, $A_{p-p} = 6.3$ nm, and $\upsilon_s = 3.3$ ms/pixel. Some of the N3 molecules which showed work function decrease are marked by arrows. (c) Cross sections determined along the lines in the images. (d) Heights of the single N3 molecules and the N3 aggregates relative to the pivalate monolayer in the topography. (e) Work function shift on the N3 molecules. Dashed lines help guide the eye.

function on these N3 molecules is smaller than that on the pivalate monolayer. The shifts of the local work function on N3 are shown in Figure 4e. Negative shifts are observed on 44% of isolated N3 molecules and 39% of the N3 aggregates. The average shifts were −0.07 and −0.04 eV for the isolated and aggregated N3 molecules, respectively. The shift on an N3 molecule was insensitive to where it adsorbed (in the middle of a terrace or at a step). The work function shifts persisted for hours and disappeared in a day, when the light was off.

The pivalate anions cannot absorb visible light. The work function of the pivalate-covered surface should be insensitive to irradiation. The photoinduced shifts of the work function, from +0.07 to −0.07 eV for the isolated N3 molecules, are related to the photoexcitation of the N3 molecules. It is unlikely that the electron distribution of the N3 molecules in the excited state makes the shifts. The lifetime of the excited N3 molecules is in a 10^{-10} s time domain, as evidenced by luminescence quenching.[30] The frequency of photoexcitation was 0.1 s^{-1} in our photon flux. When the surface is irradiated with monochromatic light of 534 nm wavelength and 1.5 mW cm^{-2} intensity, the photon flux is 3×10^{15} cm^{-2} s^{-1}. Using the absorption cross section of N3 in ethanol, 1.42×10^7 cm^2 mol^{-1} at 534 nm,[31] one N3 molecule receives 0.1 photon in 1 s.

We propose that the negative shifts of the work function result from the electron injection from the photoexcited N3 to the surface. A pair of the N3 cation and injected electron appears at the surface. The resultant dipole moment reduces the work function locally. The injected electron can be returned to the N3 cation, though. This back electron transfer should be suppressed less frequently than 0.1 s^{-1}. Otherwise, our microscope cannot observe the cation. The rate of back electron transfer has been reported to be 10^3 s^{-1}.[32−34] We need to assume electron trap sites in our dye-sensitized single crystals. One possible site is the sixfold-coordinated Ti atom bound to bridge O atoms. When a proton dissociated from pivalic acid is adsorbed on a bridge O atom, the sixfold-coordinated Ti atom is able to trap an electron.[35]

$$(CH_3)_3CCOOH + Ti^{4+}-O^{2-}-Ti^{4+} \rightarrow (CH_3)_3CCOO^- + Ti^{4+}-OH^--Ti^{4+} \quad (3)$$

$$TiO_2 + h\nu \rightarrow TiO_2 + h^+ + e^- \quad (4)$$

$$Ti^{4+}-OH^--Ti^{4+} + e^- \rightarrow Ti^{3+}-OH^--Ti^{4+} \quad (5)$$

Some N3 molecules were sensitive to light irradiation, and the others were not. This is one of the important findings of the present study. Consider possible reasons of the different responses. We proposed in the previous paragraph electron trap sites to avoid the back electron transfer. When the number of the trap sites is less than the number of N3 molecules, some N3 molecules are quickly neutralized. This may be the case here. The proposed electron trap sites, sixfold-coordinated Ti^{4+} at the surface, are ready to receive electrons provided by bridge O vacancies. Three to five percent of the bridge O atoms are usually missing on vacuum-annealed TiO_2 surfaces, and one O vacancy provides two electrons. Another possible reason is different abilities of electron injection. The injection efficiency should be sensitive to the overlap of the excited-state molecular orbital and the unoccupied surface density of states. The adsorbed N3 molecules of two different structures, for example, (i) and (ii) of Figure 1d, provide different extents of the overlap.

5.4. KPFM Measurements under Infrared Light. The visible light used to observe images of Figure 4 excites the adsorbed N3 molecules and also the Si tip of the microscope. Work function measurements were conducted under infrared light irradiation to examine the effect of the photoexcitation of the tip. The absorption edge of Si at room temperature is 1.1 eV in energy and 1.1 μm in wavelength.[36] The conduction and valence bands of n-type Si are bent downward from the surface to the bulk to make a space charge layer. When electrons and holes are photoexcited in the layer, the bent band is relaxed. The contact potential difference observed with the KPFM is possibly affected by the tip excitation.

Figure 5a and b shows the topography and local work function of the N3-adsorbed surface observed in IR light irradiation of 0.3 mW cm^{-2} intensity. The spectrum of the light is shown in

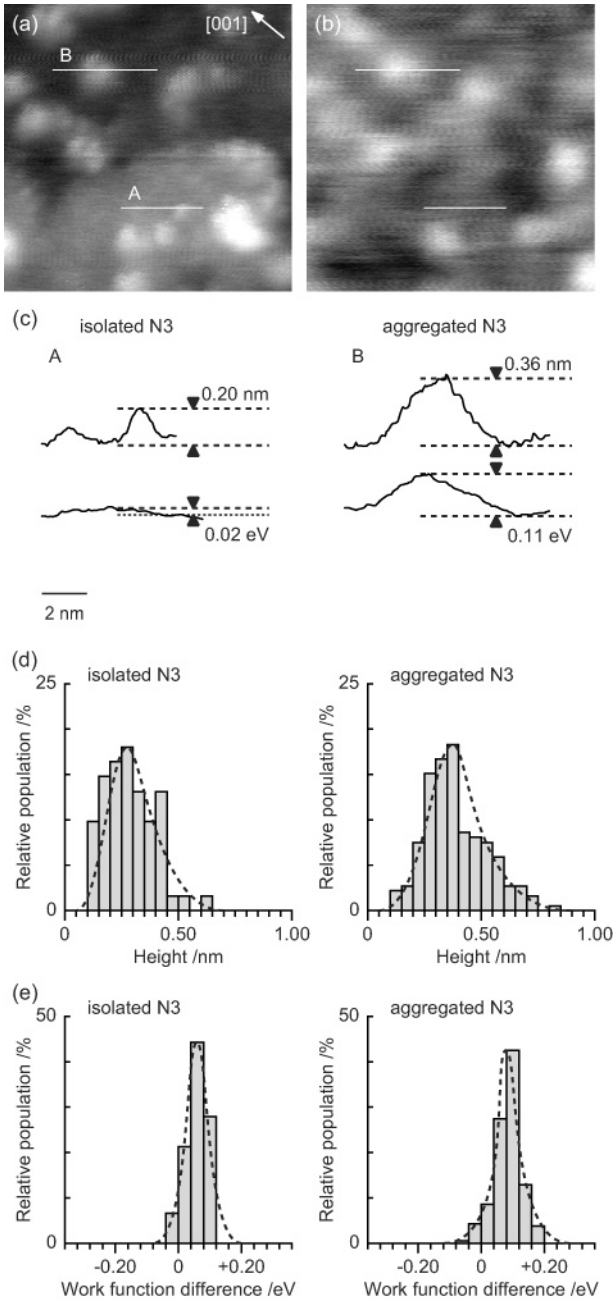

Figure 5. (a) Topography and (b) work function maps of the N3-adsorbed TiO_2 surface obtained under infrared light of 0.3 mW cm^{-2} intensity (30×30 nm^2). $\Delta f = -81$ Hz, $A_{p-p} = 6.2$ nm, and $v_s = 3.3$ ms/pixel. (c) Cross sections determined along the lines in the images. (d) Heights of the single N3 molecules and the N3 aggregates relative to the pivalate monolayer in the topography. (e) Work function perturbation on the N3 molecules. Dashed lines help guide the eye.

Figure 1e. The absorption edge of N3 is at 750 nm as seen in the spectrum of Figure 1c. The Si tip was exclusively excited with the IR light. The topography and local work function of N3 present distributions similar to those observed in the dark (Figure 3). The adsorbed N3 therefore is responsible for the work function shifts observed in visible light irradiation.

The absence of the tip-induced work function shift is due to the number of photoexcited charge carriers being much less than the number of intrinsic dopants. When the Si tip is irradiated with a photon flux F, the volume number density of photons absorbed in the layer of depth L from the surface, ρ_{abs}, is

$$\rho_{abs} = F(1 - \exp(-\alpha L))\frac{1}{L} \tag{6}$$

where α is the absorption coefficient of the incident light. ρ_{abs} goes to $F\alpha$ at the extreme of $L \rightarrow 0$. Hence, the rate of the electron−hole pair generation is $F\alpha$. On the other hand, the electrons and holes recombine along the first-order kinetics with a time constant τ. In a steady state, the recombination rate is balanced with the excitation rate. The number of electrons in the conduction band n is given as

$$\frac{n}{\tau} = F\alpha \tag{7}$$

Estimate n with the flux of IR light. With F of 10^{16} photons cm^{-2} s^{-1} and α of 10^3 cm^{-1} (ref 37) for Si, the excitation rate is 10^{19} cm^{-3} s^{-1}. The τ value of single crystalline Si is 10^{-4} s.[38] n is thus estimated to be 10^{15} cm^{-3}, which is 2 orders of magnitude less than the dopant concentration, 10^{17} cm^{-3}.

Summary

The local work function of N3 dye adsorbed on TiO_2(110) was observed with a Kelvin probe force microscope. Visible light irradiation induced a negative shift of the work function of N3, which is related to electron injection. This work provided the first measurement of the electron transport from individual dye molecules to the TiO_2 electrode.

Acknowledgment. The present work was supported in part by the New Energy and Industrial Technology Development Organization (NEDO) in association with the Ministry of Economy, Trade and Industry, Japan.

References and Notes

(1) Grätzel, M. *J. Photochem. Photobiol., A* **2004**, *164*, 3.
(2) Wang, Z.; Kawauchi, H.; Kashima, T.; Arakawa, H. *Coord. Chem. Rev.* **2004**, *248*, 1381.
(3) Chiba, Y.; Islam, A.; Watanabe, Y.; Komiya, R.; Koide, N.; Han, L. *Jpn. J. Appl. Phys.* **2006**, *45*, L638.
(4) Galoppini, E. *Coord. Chem. Rev.* **2004**, *248*, 1283.
(5) Hagfeldt, A.; Grätzel, M. *Chem. Rev.* **1995**, *95*, 49.
(6) Ishibashi, T.; Uetsuka, H.; Onishi, H. *J. Phys. Chem. B* **2004**, *108*, 17166.
(7) Sasahara, A.; Pang, C. L.; Onishi, H. *J. Phys. Chem. B* **2006**, *110*, 4751.
(8) Nonnenmacher, M.; O'Boyle, M. P.; Wickramasinghe, H. K. *Appl. Phys. Lett.* **1991**, *58*, 2921.
(9) Kitamura, S.; Iwatsuki, M. *Appl. Phys. Lett.* **1998**, *72*, 3154.
(10) *Noncontact Atomic Force Microscopy*; Morita, S., Wiesendanger, R., Meyer E., Eds.; Springer: Berlin, 2002.
(11) Sasahara, A.; Pang, C. L.; Onishi, H. *J. Phys. Chem. B* **2006**, *110*, 13453.
(12) Miyato, Y.; Kobayashi, K.; Matsushige, K.; Yamada, H. *Jpn. J. Appl. Phys.* **2005**, *44*, 1633.
(13) Sasahara, A.; Uetsuka, H.; Onishi, H. *Jpn. J. Appl. Phys.* **2004**, *43*, 4647.
(14) Eguchi, T.; Fujikawa, Y.; Akiyama, K.; An, T.; Ono, M.; Hashimoto, T.; Morikawa, Y.; Terakura, K.; Sakurai, T.; Lagally, M. G.; Hasegawa, Y. *Phys. Rev. Lett.* **2004**, *93*, 266102.
(15) Okamoto, K.; Yoshimoto, K.; Sugawara, Y.; Morita, S. *Appl. Surf. Sci.* **2003**, *210*, 128.
(16) Shiota, T.; Nakayama, K. *Jpn. J. Appl. Phys.* **2002**, *41*, L1178.
(17) Kitamura, S.; Suzuki, K.; Iwatsuki, M.; Mooney, C. B. *Appl. Surf. Sci.* **2000**, *157*, 222.
(18) Diebold, U. *Surf. Sci. Rep.* **2003**, *48*, 53.
(19) Sasahara, A.; Uetsuka, H.; Ishibashi, T.; Onishi, H. *J. Phys. Chem. B* **2003**, *107*, 13925.
(20) Hugot-Le Goff, A.; Falaras, P. *J. Electrochem. Soc.* **1995**, *142*, L38.
(21) Falaras, P.; Grätzel, M.; Hugot-Le Goff, A.; Vrachnou, E.; *J. Electrochem. Soc.* **1993**, *140*, L92.

(22) Patthey, L.; Rensmo, H.; Persson, P.; Westmermark, K.; Vayssieres, L.; Stashans, A.; Petersson, Å.; Brühwiler, P. A.; Siegbahn, H.; Lunell, S.; Mårtensson, N. *J. Chem. Phys.* **1999**, *110*, 5913.

(23) Thevuthasan, S.; Herman, G. S.; Kim, Y. J.; Chambers, S. A.; Peden, C. H. F.; Wang, Z.; Ynzunza, R. X.; Tober, E. D.; Morais, J.; Fadley, C. S. *Surf. Sci.* **1998**, *401*, 261.

(24) Fantacci, S.; Angelis, F. D.; Selloni, A. *J. Am. Chem. Soc.* **2003**, *125*, 4381.

(25) Sasahara, A.; Uetsuka, H.; Onishi, H. *J. Phys. Chem. B* **2001**, *105*, 1.

(26) Sasahara, A.; Uetsuka, H.; Onishi, H. *Phys. Rev. B* **2001**, *64*, 121406(R).

(27) Hiehata, K.; Sasahara, A.; Onishi, H. *Nanotechnology* **2007**, *18*, 0844007.

(28) Onishi, H.; Aruga, T.; Egawa, C.; Iwasawa, Y. *Surf. Sci.* **1988**, *193*, 33.

(29) Persson, P.; Lundqvist, M. J. *J. Phys. Chem. B* **2005**, *109*, 11918.

(30) Tachibana, Y.; Moser, J. E.; Grätzel, M.; Klug, D. R.; Durrant, J. R. *J. Phys. Chem.* **1996**, *100*, 20056.

(31) Fillinger, A.; Soltz, D.; Parkinson, B. A. *J. Electroanal. Chem.* **2002**, *149*, A1146.

(32) Kuciauskas, D.; Freund, M. S.; Gray, H. B.; Winkler, J. R.; Lewis, N. S. *J. Phys. Chem. B* **2001**, *105*, 392.

(33) Tachibana, Y.; Haque, S. A.; Mercer, I. P.; Durrant, J. R.; Klug, D. R. *J. Phys. Chem. B* **2000**, *104*, 1198.

(34) Takeshita, K.; Sasaki, Y.; Kobashi, M.; Tanaka, Y.; Maeda, S.; Yamakata, A.; Ishibashi, T.; Onishi, H. *J. Phys. Chem. B* **2003**, *107*, 4156.

(35) Henderson, M. A.; White, J.; Uetsuka, H.; Onishi, H. *J. Am. Chem. Soc.* **2003**, *125*, 14974.

(36) Macfarlane, G. G.; McLean, T. P.; Quarrington, J. E.; Roberts, V. *Phys. Rev.* **1958**, *111*, 1245.

(37) Dash, W. C.; Newman, R. *Phys. Rev.* **1955**, *99*, 1151.

(38) Yablonovitch, E.; Allara, D. L.; Chang, C. C.; Gmitter, T.; Bright, T. B. *Phys. Rev. Lett.* **1986**, *57*, 249.